FULL PAPER

Ultrahigh Electrical Resistance of Poly(cyclohexyl methacrylate)/Carbon Nanotube Composites Prepared Using Surface-Initiated Polymerization

Kenichi Hayashida and Hiromitsu Tanaka*

Multiwalled carbon nanotubes on which poly(cyclohexyl methacrylate)s are densely grafted (PCHMA-CNTs), are synthesized using a modified surface-initiated atom transfer radical polymerization technique. The electrical resistance of PCHMA-CNT is systematically characterized under direct current (DC) and alternating current and compared to that of conventional nanocomposites prepared by blending PCHMA with the CNT (PCHMA/CNT). At a comparable volume fraction of CNT, DC volume resistivity of PCHMA-CNT is 14 orders of magnitude higher than that of PCHMA/CNT. This is because the grafted polymer with a combination of the high molecular weight and the high grafting density isolates individual CNTs at a long distance in the PCHMA-CNT system. In addition, impedance analysis reveals that the highly insulated PCHMA-CNT has the same electrical nature as neat PCHMA, i.e., it is a dielectric. Furthermore, dynamic mechanical analysis shows PCHMA-CNT has a good mechanical properties as well as ultrahigh electrical resistance.

1. Introduction

Polymer/carbon nanotube (CNT) nanocomposite materials have been much developed over the last two decades.[1–5] The CNTs impart good mechanical properties and high electrical and thermal conductivities to polymer materials at low CNT loading. Especially for electrical conductivity, several orders of magnitude enhancement is achieved at a few vol% of CNT loading.[6–10] The polymer/CNT nanocomposites become conductive becasue of the formation of a 3D conductive network of the CNT within the polymer matrix when the CNT content exceeds a critical value, known as a percolation threshold. The percolation thresholds are typically much less than 1 vol% for the polymer/CNT composites,[1–5] whereas more than 10 vol% of loading is required for conventional conductive fillers such as carbon black. The extremely low percolation threshold for the CNT means almost all polymer/CNT nanocomposites are electrically conductive. The polymer/CNT nanocomposites, therefore, cannot be used for some applications demanding not only good mechanical properties and/or high thermal conductivity but also electrical insulation (more than 1 TΩ cm) (e.g., printed circuit boards, sealants for semiconductor devices and light emitting diodes, insulators for the coils of motors). The unavoidable electrical conductivity of the polymer/CNT nanocomposites limits the extent of the applications. Although there are numerous studies on high electrical conductivity of the polymer/CNT nanocomposites, no highly insulated polymer/CNT nanocomposite has been reported so far.

A solution to prevent the electrical conductivity of the polymer/CNT nanocomposites is that individual CNTs are completely covered with polymer matrix not to contact each other. Polymer grafting on the surface of the CNT shows promise of insulation of the CNT.[11–15] Unlike physically adsorbed polymer chain, the covalently attached polymer chain would withstand processing such as compression molding at elevated temperature. In addition, the grafting density of the polymer chain is important for high electrical resistance. When the grafting density is low, even if the molecular weight is high, the CNT might approach each other within several nanometers, as indicated by previous morphological works.[12,13] It is widely accepted that such small internanotube distance allows efficient electron hopping between the nanotubes (tunneling conduction).[16–19] In contrast, a combination of a high molecular weight and a high grafting density isolates individual CNTs at a long distance by steric repulsion of "polymer brush",[12–15] and a highly insulated polymer/CNT nanocomposite could be produced. In the last decade, surface-initiated polymerization (SIP) techniques (especially, using atom transfer radical polymerization (ATRP), which is a highly versatile technique for controlled polymerization) have been developed to provide high molecular weight polymers densely grafted on nanoparticles such as silicas,[20,21] metals, and metal oxides.[22,23] Many methods for ATRP from the surface of single-walled carbon nanotubes (SWCNTs)[24,25] and multi-walled carbon nanotubes (MWCNTs)[26–28] have been reported as well. While high molecular weight polymers of over 100k were obtained,[24] the grafting densities of the polymers were not identified for the SI-ATRP of CNTs.

Dr. K. Hayashida, Dr. H. Tanaka
Organic Materials Lab
Toyota Central R&D Labs., Inc.
Nagakute, Aichi 480-1192, Japan
E-mail: e1440@mosk.tytlabs.co.jp

DOI: 10.1002/adfm.201103089

In this paper, we demonstrate ultrahigh electrical resistance of the polymethacrylate/MWCNT nanocomposite prepared using a modified SI-ATRP technique. We have recently established an SI-ATRP method of synthesizing high molecular weight polymethacrylate densely grafted on silica nanoparticles using an originally designed ATRP initiator, *p*-(bromomethyl) benzyl 2-bromoisobutylate (BBnBiB).[15,21] Our method has been modified to be applicable to MWCNT, and the ATRP initiator moiety was covalently attached on the surface of the MWCNT. Using this ATRP initiator-modified MWCNT (CNT-Br), a series of MWCNTs on which poly(cyclohexyl methacrylate)s (PCHMAs) with various molecular weights were grafted (PCHMA-CNTs), were synthesized, and the grafting density was determined through careful characterization. We chose PCHMA as the polymethacrylate because low polarity of the cyclohexyl group is expected to impart low water absorption to the polymethacrylate; high electrical resistance is susceptible to the water absorption. Second, PCHMA has a comparatively high glass-transition temperature of 104 °C. The electrical resistance of PCHMA-CNT was systematically characterized under direct current (DC) and alternating current (AC), and compared to those of two conventional nanocomposites prepared by blending PCHMA with CNT or CNT-Br (PCHMA/CNT and PCHMA/CNT-Br). Furthermore, polymer/CNT compatibilities in the three nanocomposites were investigated using dynamic mechanical analysis. To the best of our knowledge, this is the first report on the electrical and mechanical properties of the polymer/CNT nanocomposite system in which all the polymer chains are tethered on the CNT surface.

2. Results and Discussion

ATRP-initiator modified MWCNT (CNT-Br) was synthesized as **Scheme 1**, where MWCNT with an average diameter of 10 nm was used. In the first step in Scheme 1b, the CNT was amine-functionalized using an aryl diazonium salt method developed by Tour et al.[29,30] Although amine-functionalized CNTs have been synthesized using diazonium salts prepared from *p*-phenylenediamine,[31] the diazonium salt was unstable to decompose even at 5 °C as had been pointed out by Delamar et al.[32] We have found that a diazonium salt from 4,4′-oxydianiline (ODA) was stable at 5 °C (similarly, diazonium salts prepared

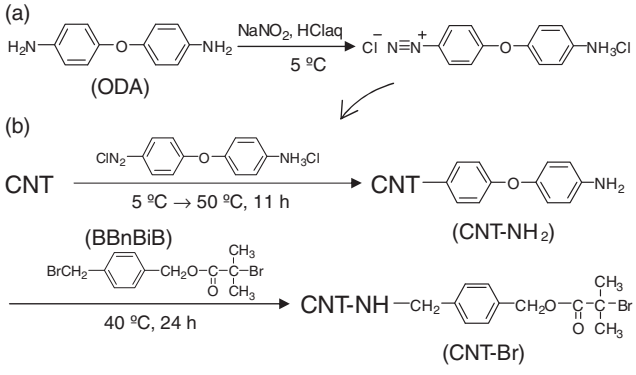

Scheme 1. Preparation of ATRP initiator-modified CNT.

Table 1. Characteristics of the Modified CNTs.

Code	CNT weight fraction[a)]	Loading [mmol g^{-1}][b)]	Element content [wt%][c)]		
			H	N	Br
CNT-NH_2	0.693	2.4	1.7 (1.8)	2.3 (2.1)	–
CNT-Br	0.664	0.23	2.2 (1.9)	2.2 (2.0)	1.2 (1.1)

[a)]Determined by the weight increment of the CNT sample after reaction; [b)]The amount of the introduced moiety per unit weight of the CNT, which was calculated from the molecular weight of the moiety and the CNT weight fraction; [c)]Estimated from the loading amounts. The value in the parentheses was obtained by elemental analysis of the modified CNTs.

from 4,4′-thiodianiline and 4,4′-diaminodiphenylmethane were stable), and efficiently reacted with the CNT at the higher temperature (Scheme 1a). Thereby, the 4-(*p*-aminophenoxy)phenyl (APP) moiety of ODA was covalently attached to the CNT surface (CNT-NH_2). We calculated the CNT weight fraction of CNT-NH_2, loading amounts of the APP moiety on the CNT and the element content of CNT-NH_2 using a weight increment of the CNT after the reaction (**Table 1**). The APP moiety attached on the CNT could not be completely and selectively decomposed in thermogravimetric analysis (Supporting Information) and elemental analysis could not distinguish a carbon atom of the APP moiety from that of the CNT. The calculated values for CNT-NH_2 in Table 1 were supported by results of elemental analysis of H, N for CNT-NH_2. The experimental H and N contents in parentheses in Table 1 are consistent with the calculated element contents from the sample weight. The APP moiety attached on the CNT was directly observed by transmission electron microscopy (TEM) (**Figure 1**b). It is confirmed that an amorphous-like layer uniformly covers the CNT surface. The thickness of the layer is approximately 1.5 nm, which indicates formation of a multilayer of the APP moiety (Supporting Information). Similar multilayers produced by diazonium salts have previously been reported.[31,33] In the second step in Scheme 1b, CNT-NH_2 was reacted with BBnBiB,[21] and the ATRP-initiator moiety was introduced on the surface (CNT-Br). CNT-Br was homogenously dispersible in *N,N*-dimethylformamide or *o*-dichlorobenzene (DCB) with the aid of sonication. The Br content in CNT-Br was confirmed by combustion ion chromatography (Table 1). Cyclohexyl methacrylate was polymerized using CNT-Br, where an unfixed initiator, benzyl 2-bromoisobutylate (BnBiB) had been added in order to obtain a free PCHMA produced from the BnBiB for molecular weight characterization. Several groups have reported that the number average molecular weights (M_n) of graft polymers were almost the same as free polymers simultaneously formed.[20,25,34] The resultant free PCHMA was separated from PCHMA-grafted CNT (CNT-PCHMA) using centrifugation. The characterization result of the free PCHMA is shown in **Table 2** together with the calculated grafting density of the tethered PCHMA on the CNT (Supporting Information). The grafted PCHMA was found to have a high grafting density of 0.14 chains nm^{-2}, enough to be referred to as "dense polymer brush".[14,35] The grafted PCHMA chain is clearly observed in the TEM image of CNT-PCHMA in Figure 1d.

For electrical and mechanical measurements, surface-initiated polymerization using CNT-Br was scaled up, and a series

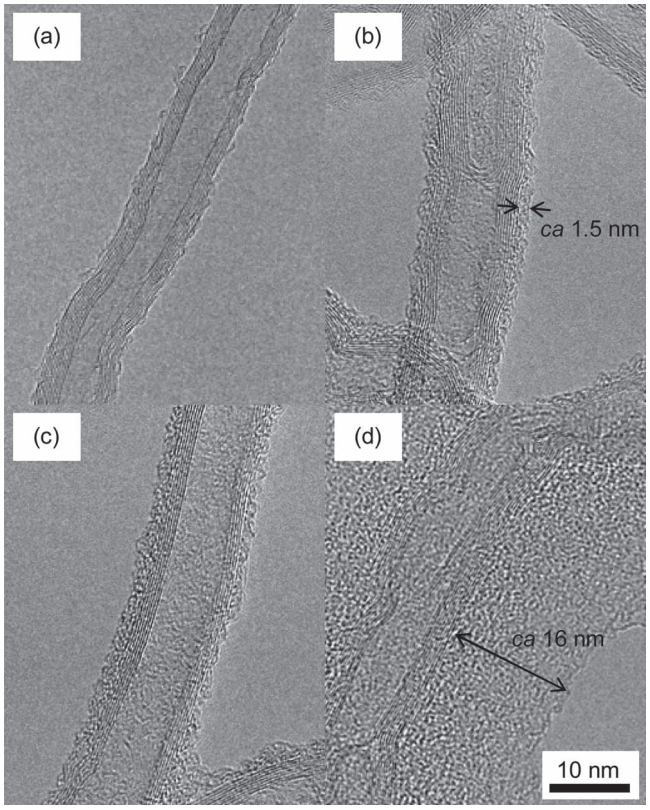

Figure 1. TEM images of the modified CNTs: a) CNT, b) CNT-NH_2, c) CNT-Br, and d) CNT-PCHMA.

Table 2. Characteristics of CNT-PCHMA

CNT weight fraction[a)]	M_n ($\times 10^{-3}$)[b)]	M_w/M_n[b)]	Loading [μmol g^{-1}][c)]	Grafting density [chains nm^{-2}][d)]
0.155	93.8	1.33	53	0.14

[a)]Determined by the weight increment of the CNT sample after polymer-grafting; [b)]Values for the free polymer grown from an unfixed initiator; [c)]The amount of the grafted polymer chains per unit weight of the CNT, which was calculated using the M_n and the CNT weight fraction; [d)]Calculated from the loading amount of the polymer chains and the specific surface area of the CNT (220 m^2 g^{-1}).

of PCHMA-CNTs with various molecular weights from 60k to 190k, were obtained as listed in **Table 3**, where the number in the sample code represents the volume fraction of CNT (Φ_{CNT}). These samples are generally soluble in whatever solvents PCHMA is soluble in. Several papers have reported orientation of CNTs dispersed in solvents under electric fields;[36–38] Because of the electric polarizability of CNT, the tube axis aligns parallel to an electric field. First, we prepared PCHMA-CNT solutions in DCB (0.1 vol% of CNT) with aid of sonication, and the stability of the solutions was checked out over a month. Some sediment was seen for PCHMA-CNT14 while PCHMA-CNT06 has shown no sedimentation because of the molecular weight as high as 190k. The stable PCHMA-CNT06 solution was sandwiched between indium tin oxide (ITO)-coated glass substrates with a gap of 100 μm, and applied AC voltages (60 Hz). **Figure 2**a shows visible absorption spectra of the CNT solution under the

Table 3. Characteristics of a Series of PCHMA-CNTs.

Code[a)]	M_n ($\times 10^{-3}$)[b)]	Fraction of CNT		Internanotube distance [nm][e)]
		weight[c)]	volume[d)]	
CNT-Br	–	0.664	0.547	–
PCHMA-CNT14	60.2	0.214	0.143	15.2
PCHMA-CNT12	72.5	0.188	0.124	17.0
PCHMA-CNT11	82.5	0.171	0.112	18.4
PCHMA-CNT09	102	0.145	0.094	21.0
PCHMA-CNT06	190	0.087	0.055	30.8

[a)]The number in the sample code represents the volume percentage of CNT; [b)]Estimated using the loading amount of the polymer chains on the CNT described in Table 2; [c)]Determined by the weight increment of the CNT sample after polymer-grafting; [d)]Calculated using a bulk density of 1.8 g cm^{-3} for the CNT and of 1.1 g cm^{-3} for the organic component; [e)]Ideal value calculated assuming CNT is hexagonally packed.

AC voltages. The absorbance is decreased with the increase of the applied voltage, suggesting the CNT is oriented parallel to the electric field. The response speed of the CNT and reproducibility are shown in Figure 2b. The PCHMA-CNT06 solution was still stable and no electric breakdown occurred during the operation with the electric field of 300 V mm^{-1}. In contrast, it is known conventional CNT suspensions cause electrical breakdown because of the percolation of the CNT. Shan et al. reported electric breakdown occurred at an electric field of 266 V mm^{-1} even in a very dilute SWCNT suspension (0.0015 vol% of CNT).[38] Our CNT solution that is stable and insulated is promising fluid for a lot of applications such as electrorheological fluids.[38–40]

Conventional nanocomposites (PCHMA/CNT and PCHMA/CNT-Br) were prepared by blending PCHMA (M_n = 250k, M_w/M_n = 1.10) with CNT or CNT-Br, which were designed to have the same Φ_{CNT} as PCHMA-CNT. These nanocomposite samples were molded by compression of 10 MPa at 130 °C prior to electrical and mechanical measurements. **Figure 3**a shows DC volume resistivity (ρ_{DC}) of the three types of nanocomposites. PCHMA/CNT has low ρ_{DC}, which is a typical conductivity for nanocomposites containing CNTs. Due to the coating of the CNT with the organic thin layer (≈2 nm), PCHMA/CNT-Br has higher ρ_{DC} than PCHMA/CNT. However, PCHMA/CNT-Br becomes conductive (ρ_{DC} of less than 10^{10} Ω cm) when Φ_{CNT} is over 0.05. In contrast, PCHMA-CNT has very high ρ_{DC} of over 100 TΩ cm even at Φ_{CNT} = 0.094. In comparison at Φ_{CNT} = 0.055, ρ_{DC} of PCHMA-CNT is 14 orders of magnitude higher than that of PCHMA/CNT. To our knowledge, such ultrahigh electrical resistance has not been reported for polymer/CNT nanocomposites. On the other hand, when Φ_{CNT} is over 0.1, ρ_{DC} of PCHMA-CNT is rapidly decreased in spite of polymer grafting. This is because tunneling conduction dominantly occurs.[16–19] In this conduction mechanism, $\ln\rho_{DC}$ is proportional to the internanotube gap width. The average gap width is proportional to $\Phi_{CNT}^{-1/3}$ due to spatial considerations. Therefore, the contribution of the tunneling conduction to ρ_{DC} is described by $\ln\rho_{DC} \propto \Phi_{CNT}^{-1/3}$.[16–18] In Figure 3b, these linear relationships are plotted for the tree types of nanocomposites.

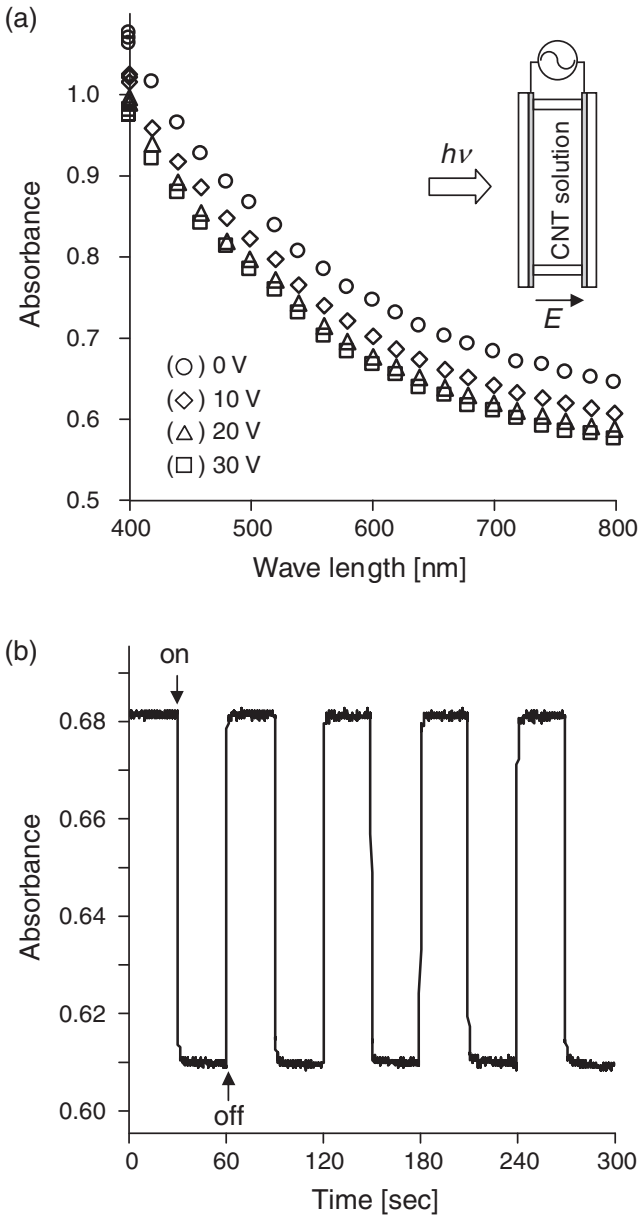

Figure 2. a) Visible absorption spectra of PCHMA-CNT06 dissolved in *o*-dichlorobenzene under applied AC voltages (60 Hz). The CNT solution was sandwiched between ITO-coated glass substrates with a gap of 100 µm. b) Response of the absorbance at 700 nm to an applied voltage between 30 V (on) and 0 V (off). The on-off switching was operated at intervals of 30 s.

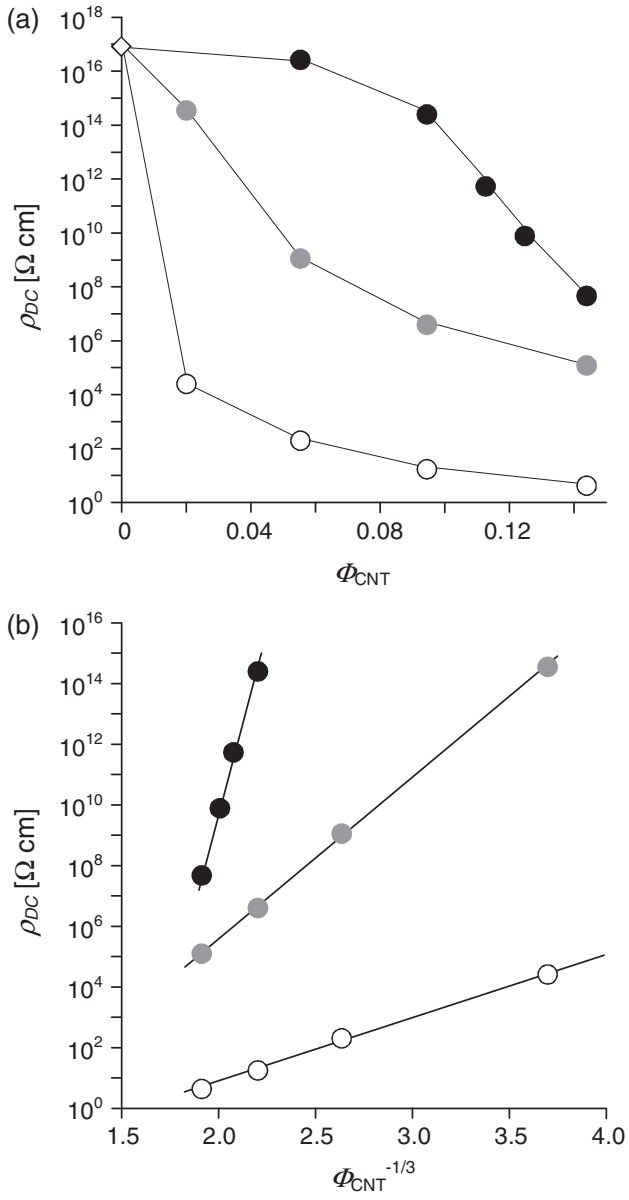

Figure 3. a) DC volume resistivity (ρ_{DC}) of PCHMA (diamond) and three series of nanocomposites (circles) as a function of volume fraction of CNT. White circles, PCHMA/CNT; gray circles, PCHMA/CNT-Br; black circles, PCHMA-CNT. b) Plot of log ρ_{DC} versus $\Phi_{CNT}^{-1/3}$.

The slope of the relationship for PCHMA-CNT is greater than those for PCHMA/CNT-Br and PCHMA/CNT, suggesting the average gap width in the PCHMA-CNT system is greater.[18] This result strongly supports the CNTs cannot come close each other in the PCHMA-CNT system because of the polymer brush on the CNT surface. The ideal gap width is calculated and shown in Table 3, assuming that the CNT is hexagonally packed in the PCHMA-CNT system. Note that we obviously overestimate the internanotube distance, considering the actual random packing of the CNT in the PCHMA-CNT system.

AC resistance, impedance (Z), depends on the frequency (f) of an applied electric field. The magnitude of the impedance, $|Z|$ for the nanocomposites with $\Phi_{CNT} = 0.094$ is plotted as a function of f in the range of 100 Hz to 10 MHz in **Figure 4**a. In the log–log plot, $|Z|$ of PCHMA-CNT09 is decreased linearly with the increase in f similar to that of PCHMA, which suggests PCHMA-CNT09 has the same electrical nature as PCHMA. In the case of PCHMA/CNT-Br, $|Z|$ is almost independent of f in the range of 100 Hz to 1 kHz, but decreased in the higher frequency. $|Z|$ of PCHMA/CNT is independent of f in all the frequency range, which is a typical conductor behavior. These electrical properties of nanocomposites are characterized in detail

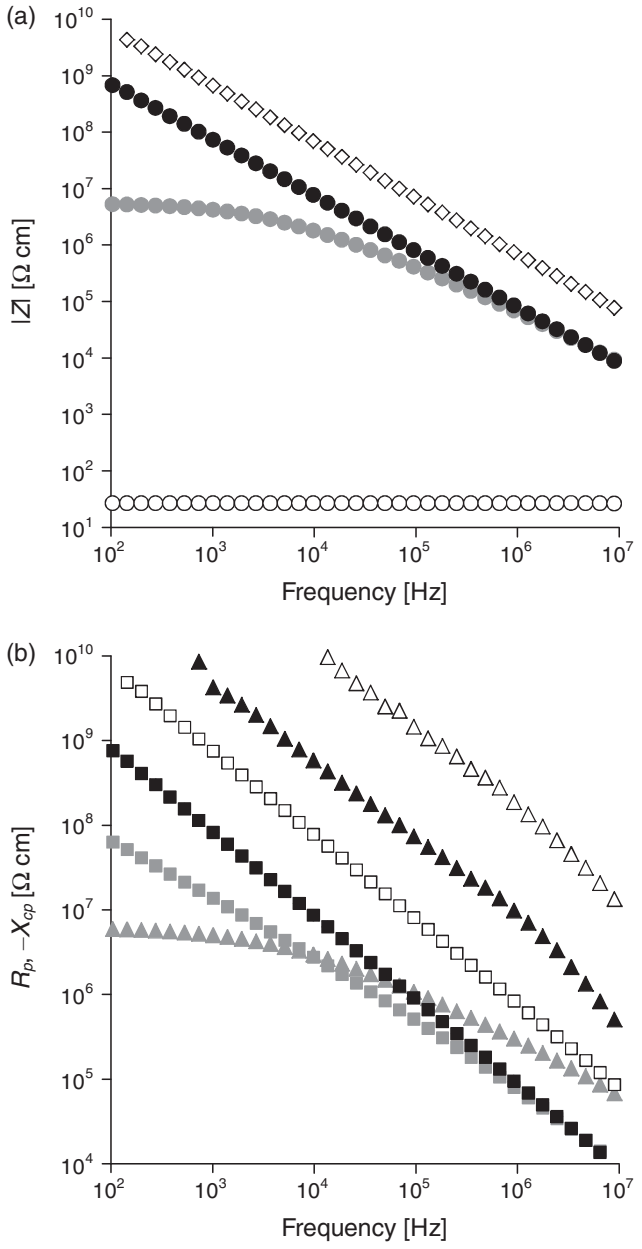

Figure 4. a) Frequency dependence of magnitude of impedance (|*Z*|) of PCHMA (diamond) and three types of nanocomposites (circles). White circles, PCHMA/CNT09; gray circles, PCHMA/CNT-Br09; black circles, PCHMA-CNT09. b) Resistance (R_p, triangle) and capacitive reactance (X_{cp}, square) components separated from *Z* under a parallel resistor-capacitor circuit. White symbols, PCHMA; gray symbols, PCHMA/CNT-Br09; black symbols, PCHMA-CNT09.

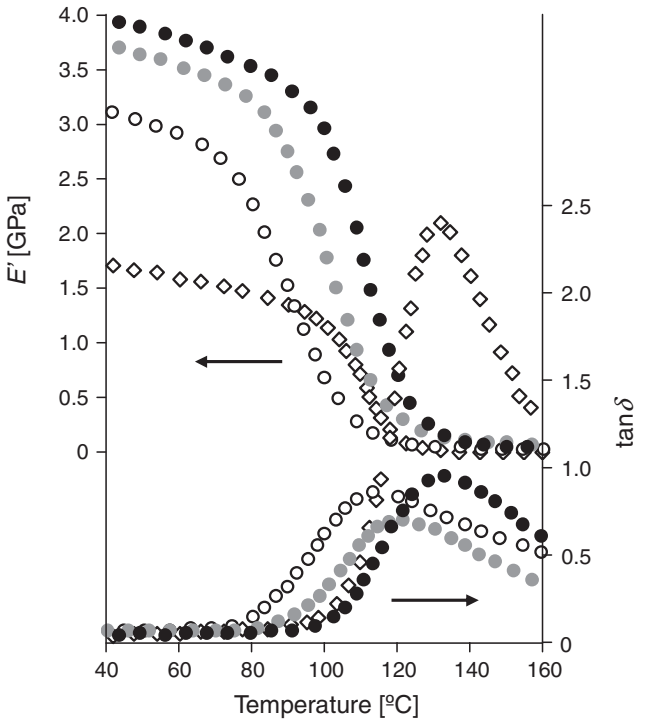

Figure 5. Temperature dependence of storage modulus (*E'*) and loss tangent (tan δ) of PCHMA (diamond) and three types of nanocomposites (circles) at 1 Hz. White circles, PCHMA/CNT09; gray circles, PCHMA/CNT-Br09; black circles, PCHMA-CNT09.

using impedance analysis. The nanocomposites are simply modeled as circuits of a resistor and a capacitor connected in parallel, where *Z* is divided into the resistance (R_p) and the capacitive reactance (X_{cp}) by the following equation, $1/Z = 1/R_p + 1/(jX_{cp})$; *j* is the imaginary unit. The two components, R_p and $-X_{cp}$ for our nanocomposites are shown in Figure 4b. Notice that X_{cp} has a minus sign. For PCHMA-CNT, $-X_{cp}$ is much smaller than R_p in all the frequency range, which shows in the parallel resistor-capacitor circuit, almost all electrical current is passed through the capacitor. In other words, PCHMA-CNT09 is a dielectric. In the case of PCHMA/CNT-Br, a transition from a conductor ($R_p < -X_{cp}$) to a dielectric ($R_p > -X_{cp}$) is observed at ≈10 kHz.

For polymer/CNT nanocomposites, the interfaces between the matrix polymers and the CNTs play a dominant role in mechanical properties.[1–3] Strong interaction at the interface often provides good mechanical properties; stiffness, tensile and impact strengths. We investigated dynamic viscoelastic behavior of our nanocomposites. **Figure 5** shows storage modulus (*E'*and loss tangent (tan δ) curves of the three types of nanocomposites at $\Phi_{CNT} = 0.094$ as a function of temperature. As expected from the covalent bonding between the polymer chain and the CNT, PCHMA-CNT exhibits the highest *E'*of the three composites. The *E'*curve of PCHMA/CNT-Br is indicative of the improved interface relative to that of PCHMA/CNT. The compatibility between the polymer and the CNT is also evaluated from the tan δ curve. A primary dispersion peak, which is related to the glass-transition of a nanocomposite, is shifted to lower or higher temperature depending on the polymer/nanofiller compatibility. The large filler-polymer interfacial area in the nanocomposite often brings a significant change to the polymer mobility and affected the T_g.[41,42] The primary dispersion peaks of PCHMA/CNT and PCHMA/CNT-Br are located in lower temperature than that of PCHMA, suggesting poor polymer/CNT compatibilities,[41] whereas the peak top temperature for PCHMA-CNT is shifted slightly higher temperature.

In summary, we have synthesized a series of MWCNTs on which poly(cyclohexyl methacrylate)s (PCHMAs) with various molecular weights were densely grafted (PCHMA-CNTs), using a modified SI-ATRP technique. The grafted PCHMA was found to have a high grafting density of 0.14 chains nm^{-2}, which is enough to be referred to as "dense polymer brush". PCHMA-CNT has ultrahigh electrical resistance when M_n of the grafted PCHMA exceeds 100k ($\Phi_{CNT} < 0.1$); At $\Phi_{CNT} = 0.055$, DC volume resistivity of PCHMA-CNT is 14 orders of magnitude higher than that of a conventional nanocomposite (PCHMA/CNT). This is because the polymer brush with a combination of the high molecular weight and the high grafting density isolates individual CNTs at a long distance in the PCHMA-CNT system. In addition, impedance analysis reveals the highly insulated PCHMA-CNT has the same electrical nature as neat PCHMA, i.e., it is a dielectric. Furthermore, dynamic mechanical analysis shows PCHMA-CNT has a good mechanical property as well as the ultrahigh electrical resistance.

3. Experimental Section

Preparation: MWCNTs with an average diameter and length of 10 nm and 1.5 μm, respectively, were obtained from Nanocyl SA. The density of the MWCNT was about 1.8 g cm^{-3}. The specific area was determined to be 220 m^2 g^{-1} using a standard BET method. Procedures for modification of the MWCNT were as follows:

Amine-modified CNT (CNT-NH_2): 4,4′-Oxydianiline (ODA) (12.5 g, 62.5 mmol) was dissolved in water (150 mL) containing concentrated hydrochloric acid (18.0 mL, 210 mmol) and cooled at around 5 °C. Sodium nitrite (4.40 g, 63.8 mmol) dissolved in water (50 mL) was added portionwise. After stirring for 0.5 h, the solution was added to a dispersion of MWNTs (4.00 g) in a mixture of *N,N*-dimethylformamide (DMF) (500 mL) and water (300 mL). The dispersion was sonicated and heated gradually until 50 °C for 11 h. After the reaction, triethylamine was added to convert the aromatic amine HCl salt into a free aromatic amine. The amine-modified CNT was purified by three cycles of filtration and redispersion in DMF. The purified amine-modified amine was dried at 80 °C for 3 h under vacuum. The yield was 5.77 g.

ATRP initiator-modified CNT (CNT-Br): *p*-(Bromomethyl)benzyl 2-bromoisobutylate (3.5 g, 10 mmol) and proton-sponge (0.86 g, 4.0 mmol) were added to a dispersion of CNT-NH_2 (5.64 g) in *N,N*-dimethylacetamide (DMAc) (340 mL). The mixture was sonicated and kept at 40 °C for 24 h. The initiator-modified CNT was purified by three cycles of filtration and redispersion in DMAc. The yield was 5.89 g.

PCHMA-grafted CNT (CNT-PCHMA and a series of PCHMA-CNT composites): For the synthesis of CNT-PCHMA, the surface-initiated polymerization was carried on in the presence of an unfixed initiator, benzyl 2-bromoisobutylate (BnBiB). A solution of BnBiB (0.45 μL, 2.5 μmol) in DMAc (20 mL) was added to CNT-Br (0.188 g) and CuBr (7.2 mg, 50 μmol) in a vacuum. After sonication of the mixture, 2,2′-bipyridyl (bpy) (15.6 mg, 100 μmol) in cyclohexyl methacrylate (10 mL, CHMA) was added, and the solution was kept at 60 °C for 6 h. The resultant polymer mixture was precipitated in methanol, and the free polymer grown from the unfixed initiator was separated by two cycles of dissolving in benzene and centrifugation. A series of PCHMA-CNT composites were synthesized as mentioned above except that the polymerization was scaled up and carried on in the absence of BnBiB.

Measurements: The modified CNTs were observed using a transmission electron microscope (JEOL, JEM-2100F) operated at an accelerating voltage of 200 kV. Molecular weight characterization was carried out using a size exclusion chromatograph system (Tosoh, HLC-8120GPC) equipped with a set of two separation columns of 300 mm × 7.8 mm inner diameter (Tosoh, TSKgel GMH_{HR}-H), a refractive detector, and a MALLS photometer (DAWN HELEOS, Wyatt Technology), where tetrahydrofuran (THF) was used as the eluent at a flow rate of 1.0 mL min^{-1}. The absolute molecular weights of PCHMA are calculated using the refractive index increment (dn/dc) of PCHMA (dn/dc = 0.101 mL g^{-1}). Visible absorption spectra were recorded using a UV-vis spectrophotometer (SHIMADZU, UV-2100). High DC resistance (>1 MΩ) was measured using a megohmmeter (SM-8220, Hioki) and low DC resistance (<1 MΩ) was done using a multimeter. Nanocomposites were molded into 15 mm square specimens with a thickness of ≈1 mm by compression of 10 MPa at 130 °C. Two gold electrodes 11 mm square were deposited on the top and bottom of the specimen at a distance of 2 mm from the edge of the specimen. Impedance was measured using an impedance analyzer (Agilent, 4194A) in the frequency range of 10^2 Hz to 10^7 Hz. Dynamic viscoelastic behaviors of samples molded into specimens of 20 mm × 5 mm and about 0.5 mm in thickness were investigated using a dynamic mechanical analyzer (IT Keisokuseigyo, DVA-220) at a frequency of 1 Hz and a strain amplitude of 0.02% with a heating rate of 4 °C min^{-1}.

Supporting Information

Supporting Information is available from the Wiley Online Library or from the author.

Acknowledgements

TEM observations and combustion ion chromatography were carried out by Mr. Noritomo Suzuki and Mr. Satoru Kosaka at Toyota Central R&D Labs Inc., respectively, and the authors appreciate their help.

Received: December 20, 2011
Revised: February 3, 2012
Published online: March 26, 2012

[1] J. N. Coleman, U. Khan, Y. K. Gun'ko, *Adv. Mater.* **2006**, *18*, 689.
[2] M. Moniruzzaman, K. I. Winey, *Macromolecules* **2006**, *39*, 5194.
[3] W. Bauhofer, J. Z. Kovacs, *Comp. Sci. Technol.* **2009**, *69*, 1486.
[4] Z. Spitalsky, D. Tasis, K. Paragelis, G. Costas, *Prog. Polym. Sci.* **2010**, *35*, 357.
[5] M. T. Byrne, Y. K. Gun'ko, *Adv. Mater.* **2010**, *22*, 1672.
[6] J. Sandler, M. S. P. Shaffer, T. Prasse, W. Bauhofer, K. Schulte, A. H. Windle, *Polymer* **1999**, *40*, 5967.
[7] F. Du, R. C. Scogna, W. Zhou, S. Brand, J. E. Fischer, K. I. Winey, *Macromolecules* **2004**, *37*, 9048.
[8] J. Li, P. C. Ma, W. S. Chow, C. K. To, B. Z. Tang, J.-K. Kim, *Adv. Funct. Mater.* **2007**, *17*, 3207.
[9] H. Deng, T. Skipa, E. Bilotti, R. zhang, D. Lellinger, L. Mezzo, Q. Fu, I. Alig, T. Peijs, *Adv. Funct. Mater.* **2010**, *20*, 1424.
[10] Y. Y. Huang, E. M. Terentjev, *Adv. Funct. Mater.* **2010**, *20*, 4062.
[11] C. M. Homenick, G. Lawson, A. Adronov, *Polym. Rev.* **2007**, *47*, 265.
[12] L. Yezek, W. Schartl, Y. Chen, Y. K. Gohr, M. Schmidt, *Macromolecules* **2003**, *36*, 4226.
[13] P. Akcora, H. Liu, S. K. Kumar, J. Moll, Y. Li, B. C. Benicewicz, L. S. Schadler, D. Acehan, A. Z. Panagiotopoulos, V. Pryamitsyn, V. Ganesan, J. Ilavsky, P. Thiyagarajan, R. H. Colby, J. F. Douglas, *Nat. Mater.* **2009**, *8*, 354.
[14] Y. Tsujii, K. Ohno, S. Yamamoto, A. Goto, T. Fukuda, *Adv. Polym. Sci.* **2006**, *197*, 1.
[15] K. Hayashida, H. Tanaka, O. Watanabe, *Polym. Int.* **2011**, *60*, 1194.
[16] M. T. Connor, S. Roy, T. A. Ezquerra, F. J. Balta Calleja, *Phys. Rev. B* **1998**, *57*, 2286.
[17] B. E. Kilbride, J. N. Coleman, J. Fraysse, P. Fournet, M. Cadek, A. Drury, S. Hutzler, S. Roth, W. J. Blau, *J. Appl. Phys.* **2002**, *92*, 4024.

[18] H.-C. Li, S.-Y. Lu, S.-H. Syue, W.-K. Hsu, S.-C. Chang, *Appl. Phys. Lett.* **2008**, *93*, 033104.
[19] J. Fritzsche, H. Lorenz, M. Kluppel, *Macromol. Mater. Eng.* **2009**, *294*, 551.
[20] K. Ohno, T. Morinaga, K. Koh, Y. Tsujii, T. Fukuda, *Macromolecules* **2005**, *38*, 2137.
[21] K. Hayashida, H. Tanaka, O. Watanabe, *Polymer* **2009**, *50*, 6228.
[22] K. Ohno, K.-M. Koh, Y. Tsujii, T. Fukuda, *Macromolecules* **2002**, *35*, 8989.
[23] I. Garcia, N. E. Zafeiropoulos, A. Janke, A. Tercjak, A. Eceiza, M. Atamm, I. Mondragon, *J. Polym. Sci. Part A Polym. Chem.* **2007**, *45*, 925.
[24] Z. Yao, N. Bradiy, G. A. Botton, A. Adronov, *J. Am. Chem. Soc.* **2003**, *125*, 16015.
[25] S. Qin, D. Qin, W. T. Ford, D. E. Resasco, J. E. Herrera, *Macromolecules* **2004**, *37*, 752.
[26] D. Baskaran, J. W. Mays, M. S. Bratcher, *Angew. Chem. Int. Ed.* **2004**, *43*, 2138.
[27] H. Kong, C. Gao, D. Yan, *Macromolecules* **2004**, *37*, 4022.
[28] D. Priftis, G. Sakellariou, D. Baskaran, J. W. Mays, N. Hadjichristidis, *Soft Matter* **2009**, *5*, 4272.
[29] J. L. Bahr, J. M. Tour, *Chem. Mater.* **2001**, *13*, 3823.
[30] A. D. Christopher, J. M. Tour, *Nano Lett.* **2003**, *3*, 1215.
[31] P. Viel, X. T. Le, V. Huc, J. Bar, A. Benedetto, A. L. Goff, A. Filoramo, D. Alamarguy, S. Noel, L. Baraton, P. Serge, *J. Mater. Chem.* **2008**, *18*, 5913.
[32] M. Delamar, G. Desarmot, O. Fagebaume, R. Hitmi, J. Pinson, J.-M. Saveant, *Carbon* **1997**, *35*, 801.
[33] J. Lyskawa, D. Belanger, *Chem. Mater.* **2006**, *18*, 4755.
[34] T. von Werne, T. E. Pattern, *J. Am. Chem. Soc.* **2001**, *123*, 7497.
[35] W. J. Brittain, S. A. Minko, *J. Polym. Sci. Part A Polym. Chem.* **2007**, *45*, 3505.
[36] J. Bubke, H. Gnewuch, M. Hempstead, J. Hammer, M. L. H. Green, *Appl. Phys. Lett.* **1997**, *71*, 1906.
[37] X. Q. Chen, T. Saito, H. Yamada, K. Matsushige, *Appl. Phys. Lett.* **2001**, *78*, 3714.
[38] C. Lin, J. W. Shan, *Phys. Fluids* **2007**, *19*, 121702.
[39] H. J. Choi, M. S. Jhon, *Soft Matter* **2009**, *5*, 1562.
[40] J. Yin, X. Zhao, *Nanoscale Res. Lett.* **2011**, *6*, 256.
[41] Y. Sun, Z. Zhang, K.-S. Moon, C. P. Wong, *J. Polym. Sci. Part B Polym. Phys.* **2004**, *42*, 3849.
[42] A. Bansal, H. Yang, C. Li, K. Cho, B. C. Benicewicz, S. K. Kumar, L. S. Schadler, *Nat. Mater.* **2005**, *4*, 693.